OPUS-HSO

Repositorium der Hochschule Offenburg
https://opus.hs-offenburg.de

HOCH SCHULE OFFEN BURG

Measurement Concept for the Deflection Behaviour of Shape Memory Alloy Actuators in Robotics

Alexander Dierle, Thomas Wendt, Thomas Seifert

Zitiervorschlag im APA Stil:

Dierle, A., Wendt, T., & Seifert, T. (2026). Measurement Concept for the Deflection Behaviour of Shape Memory Alloy Actuators in Robotics. *23. ITG/GMA-Fachtagung Sensoren und Messsysteme 2026*, *23*, 589–593. https://doi.org/10.5162/sensoren2026/P20

Abstract

In this paper, a combined measurement concept for characterizing a structurally integrated shape memory alloy actuator is described. The temperature-induced bending movement is measured without contact using a 3D laser line sensor, while the activation and transformation state is determined in parallel via the electrical resistance of the embedded shape memory wire. Supplementary simulations are utilised to evaluate the anticipated actuator dynamics and the viability of the measurement concept.

Nutzungsbedingungen

Dieses Dokument wird unter diesen Bedinungen zur Verfügung gestellt:
Urheberrechtlich geschützt
Für weitere Informationen siehe:
https://rightsstatements.org/page/InC/1.0/

Kontakt

Hochschule Offenburg | Bibliothek
Badstraße 24
77652 Offenburg
Telefon: (0781) 205-240
E-Mail: bibliothek@hs-offenburg.de
www.hs-offenburg.de/bibliothek

10.5162/sensoren2026/P20

Measurement Concept for the Deflection Behaviour of Shape Memory Alloy Actuators in Robotics

Alexander Dierle[1], *Thomas M. Wendt* [1] *and Thomas Seifert*[1]
[1] Offenburg University of Applied Sciences, Badstraße 24, 77652 Offenburg, Germany
alexander.dierle@hs-offenburg.de

Summary: In this paper, a combined measurement concept for characterizing a structurally integrated shape memory alloy actuator is described. The temperature-induced bending movement is measured without contact using a 3D laser line sensor, while the activation and transformation state is determined in parallel via the electrical resistance of the embedded shape memory wire. Supplementary simulations are utilised to evaluate the anticipated actuator dynamics and the viability of the measurement concept.

Keywords: Shape memory alloys, laser line sensor, actuator, additive manufacturing, robotics

Introduction and motivation

Shape memory alloys (SMAs) are considered to be among the so-called 'smart materials' and are increasingly being used in robotics and automation. This is due to the reversible martensite-austenite transformation that these alloys exhibit, which enables compact actuator designs with high energy density [1], [2], [3]. When compared with conventional drives, SMA actuators enable lightweight, low-noise and miniaturized systems that are particularly suitable for integrated gripping mechanisms, medical applications and micro-robotic structures [1]. The technological and economic relevance of these actuators is reflected in a projected annual market growth of 13.4% until 2031 [4].

The temperature-dependent bending behaviour of the structure is of central importance for the development of reliable actuator systems, as it directly reflects the transformation state of the alloy [1]. Despite the growing prevalence of SMA actuators, there are no standardised procedures that enable reproducible measurement of both deflection and phase state (cf. [5], [6], [7]). Current measurement methods, such as marker-based optical systems or point displacement sensors, often only provide local information, are susceptible to interference, or do not allow time-resolved reconstruction of the entire bending shape (cf. [5], [6], [7]).

This study provides a proof-of-concept through numerical simulation, analyzing the expected performance and sensitivity of the integrated SMA actuator measurement system before physical implementation. The combined measurement strategy presented addresses existing shortcomings in terms of resolution, reproducibility and temporal dynamics and creates the basis for a standardisable characterisation of SMA actuators. The measurement setup, data evaluation and supplementary simulations describing the expected bending behaviour and material-specific characteristic curves for the integrated actuator are described later in the paper.

Method

Based on the previous work of the authors [8], the actuator is modelled as an additively manufactured structure made of an elastic, temperature-resistant material (TPU 85A). A 40 mm long shape memory wire with a diameter of 0.5 mm is embedded in this structure during the manufacturing process. The wire is positioned 0.75 mm above the neutral axis. The temperature-induced contraction of the shape memory wire by 3.25% results in a defined bending of the structure due to the eccentric wire position. The structure has a width of 5.0 mm, a height of 4.5 mm and a length of 40 mm. The chosen geometry represents a compromise: thinner wires ($<$0.5 mm) enable shorter activation times but are mechanically unstable, while thicker wires ($>$0.5 mm) react more slowly thermally and are more difficult to activate. Lengths greater than 40 mm increase the absolute deflection, but result in lower bending stiffness and increased deflection due to their own weight. The actuator described is shown in Figure 1.

The following describes the proposed experimental measurement concept. The thermal activation of the SMA wire or actuator would be achieved by resistance-based heating with a constant heating current of 4 A. The electrical resistance of the wire would be determined by measuring the voltage drop at constant current using a four-wire measurement and would be used as a material-specific indicator of the temperature and transformation state. The choice of a heating current of 4 A is based on common recommendations and manufacturer specifications for NiTi shape memory wires (cf. [9], [10]). In this way, the temperature- and transformation-dependent state of the material can be characterised in a material-specific manner and without

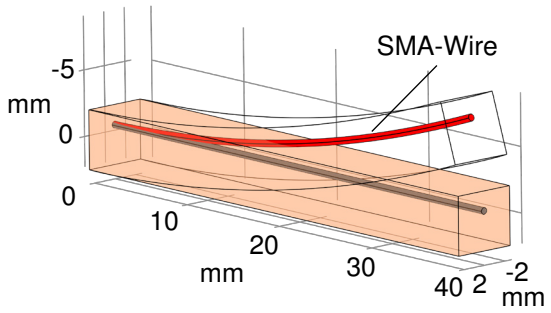

Fig. 1: Representation of the SMA actuator (red SMA-wire: activated state; grey SMA-wire: idle state)

additional sensor embedding [11], [12].

Electrical resistance is not understood as a direct temperature measurement variable, but rather as a material-specific state variable that maps the activation and transformation state via a previously determined resistance-temperature or resistance-phase characteristic curve.

A SmartRay ECCO 75.100 3D laser line sensor is proposed for the experimental acquisition of the resulting deflection profile. Its lateral resolution of 42–70 µm and vertical resolution of 5–12 µm enable a complete, time-resolved reconstruction of the bending shape with sampling rates of up to 4 kHz [13]. By linking the modelled deflection curve with the measured change in resistance, a curvature-temperature characteristic curve specific to the respective shape memory alloy can be derived. The schematic measurement setup is shown in Figure 2.

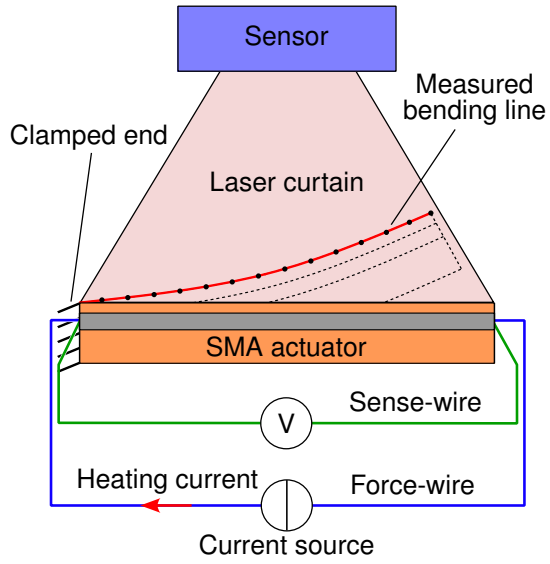

Fig. 2: Sketch of the described measurement setup

A finite-element simulation model of the considered actuator is employed to analyse deflection, curvature, and electrical resistance, as well as to evaluate the proposed measurement concept. The model is constructed in COMSOL Multiphysics and is based on the implemented Lagoudas shape memory alloy model. Since COMSOL does not allow direct implementation of the two-way effect, this is approximated using a user-defined relationship that describes the transformation-induced strain ϵ^{tr} as a function of the martensite fraction ξ. The martensite fraction ξ evolves based on the temperature field and the total stress tensor [15]. $\epsilon^{tr,max}$ denotes the maximum transformation strain.

$$\boldsymbol{\varepsilon}^{tr} = (1-\xi)\,\varepsilon^{tr,\max}\,\mathbf{e}_z \otimes \mathbf{e}_z \tag{1}$$

The martensite fraction ξ is dimensionless and takes values in the range $0 \leq \xi \leq 1$. When ξ = 1, the microstructure is completely martensitic, while when ξ = 0, it is completely austenitic.

The model described in [14] is used to estimate the electrical resistance. The stress-dependent term is neglected in the present design model. This is justified by the high compliance of the surrounding TPU structure compared to the shape memory wire

Young's modulus of structure $\ll$ Young's modulus of wire,

so that the thermally induced length change of the wire is predominantly absorbed by structural deformation (bending). The mechanical stresses arising in the wire are assumed to be small compared to the temperature- and phase-dependent contributions to resistivity. Thus, the following approximation applies:

$$\sigma\frac{\partial\rho_M}{\partial\sigma} = \sigma\frac{\partial\rho_A}{\partial\sigma} \approx 0. \tag{2}$$

The specific electrical resistance of the wire $\rho(T)$ is determined using a phase-weighted mixing rule,

$$\rho(T) = \rho_M(T)\,\xi + \rho_A(T)\,\big(1-\xi\big) \tag{3}$$

where ρ_A and ρ_M are the specific electrical resistance of the austenite and the martensite phase, respectively.

The temperature-dependent specific resistances of the martensite and austenite phases are assumed to be linear in a first approximation and described as follows:

$$\rho_M(T) = \rho_{0M} + (T - T_{0M})\frac{\partial\rho_M}{\partial T}, \tag{4}$$

$$\rho_A(T) = \rho_{0A} + (T - T_{0A})\frac{\partial\rho_A}{\partial T}. \tag{5}$$

ρ_{0M} and ρ_{0A} represent the nominal specific resistances of the martensitic and austenitic phases at the corresponding measurement temperatures T_{0M} and T_{0A}.

The electrical resistance of the shape memory wire is described by its specific electrical resistivity. Literature values according to [14], which

Tab. 1: Material parameter Nitinol/ TPU 85A [8], [14]

Material parameter	Nitinol	TPU 85A
Reference temperature	20 °C	20 °C
Poisson's ratio (ν)	0.33	0.45
Density (ρ)	6450 kg/m^3	1114 kg/m^3
Young's modulus (E)	-	20 MPa
Young's modulus (martensite) (E_M)	28 GPa	-
Young's modulus (austenite) (E_A)	78 GPa	-
Maximum transformation strain ($\epsilon^{tr,max}$)	-3.25%	-
Martensite start/ finish temp. (M_s/ M_f)	66.42 °C/ 45.67 °C	-
Austenite start/ finish temp. (A_s/ A_f)	56.99 °C/ 74.48 °C	-
Thermal conductivity (k)	18 W/(m · K)	-
Linear temp. dep. spec. resistance (martensite) ($\frac{\partial \rho_M}{\partial T}$)	1.099 · 10^{-9} (Ωm)/K	-
Linear temp. dep. spec. resistance (austenite) ($\frac{\partial \rho_A}{\partial T}$)	1.436 · 10^{-10} (Ωm)/K	-
Nominal spec. resistance (martensite) (ρ_{0M})	9.10 · 10^{-7} Ωm	-
Nominal spec. resistance (austenite) (ρ_{0A})	8.63 · 10^{-7} Ωm	-
Meas. temp. spec. resistance (martensite) (T_{0M})	0 °C	-
Meas. temp. spec. resistance (austenite) (T_{0A})	225 °C	-

are originally specified for certain wire geometries, are converted into specific resistances for this purpose. This allows the electrical behaviour to be represented in the model independently of the wire geometry. However, it should be noted that these parameters are only valid for the alloy under consideration and must be experimentally redetermined for each shape memory alloy that is actually investigated. The material and model parameters used for the simulation are summarised in Table 1.

Results

To evaluate the feasibility of the proposed measurement concept, a simulation-based analysis was conducted. The results presented in this section are derived from the simulation model utilizing the model parameters defined in the previous section (see Table 1) to establish a baseline for the expected sensor characteristics and to quantify the coupling between deflection and transformation state. The heating of the SMA wire embedded in the structure occurs with a time delay compared to the manufacturer's specifications, as the surrounding structure must also be heated in addition to the wire. The temporal progression of the calculated average wire temperature is shown in Figure 3. After 0.68 s, the wire reaches the austenite start temperature A_s = 57.0 °C, thereby initiating the phase transformation from martensite to austenite. Complete austenitisation is achieved after 1.68 s at an average wire temperature of 74.6 °C, slightly above the stress-free value A_f = 74.48 °C from Table 1 due to the tensile stress in the constrained wire and the averaging over a non-uniform temperature field. The temperature rise across the transformation range thus extends over 1.0 s, which is reflected in the slope of the temperature curve.

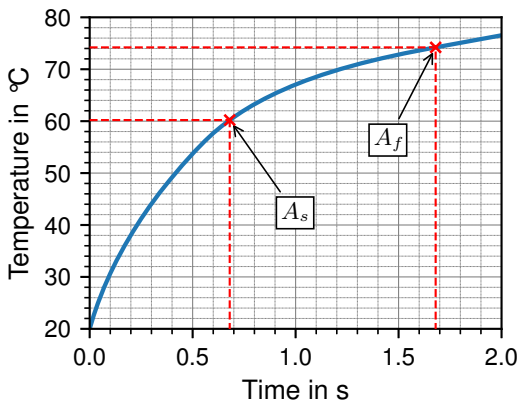

Fig. 3: The time-dependent change in the average temperature of the SMA wire embedded in the structure

The temperature-induced phase transformation results in an increasing bending of the actuator. The calculated maximum deflection at the end of the actuator is 7.05 mm and is reached at an average wire temperature of 74.6 °C, at which point the phase transformation is complete. The start of the bending coincides with the austenite

start temperature of 57.0 °C. The deflection profile of the activated SMA actuator, relative to the top of the actuator, is shown in Figure 4.

The corresponding calculated resistance behaviour of the modelled SMA alloy is shown in Figure 5. Before the phase transformation begins, the resistance increases with temperature due to the temperature dependence of the electrical resistivity of the martensitic phase. At the start of the phase transformation at the austenite start temperature A_s = 57.0 °C, a maximum resistance of 198.1 mΩ is reached. The subsequent characteristic drop in resistance marks the beginning of the phase transformation. As austenitisation progresses, the resistance continues to decrease until a minimum of 171.3 mΩ is reached at complete transformation (A_f). As the temperature continues to rise, the resistance then increases linearly again (to 172.2 mΩ at 100 °C), which is due to the temperature-dependent electrical conductivity of the austenitic phase.

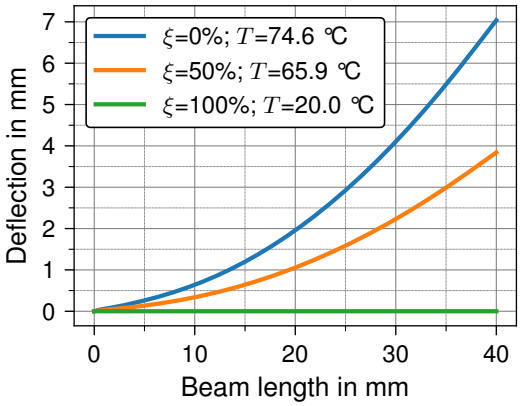

Fig. 4: Actuator deflection at different wire temperatures

Discussion

The results show that the temperature-induced phase transition of the embedded shape memory wire is consistently converted into a mechanical bending movement of the structure. The temporal course of the transition and the resulting deflection are within realistic ranges and confirm the basic functionality of the selected actuator concept.

On this thermo-mechanical basis, the simulation allows the electrical resistance measurement to be evaluated as an indirect state variable. The characteristic curve of the resistance signal in the transformation range shows the start of activation and the completed transformation state. The decisive factor here is not the absolute resistance value, but the reproducible signal shape in relation to the transformation state,

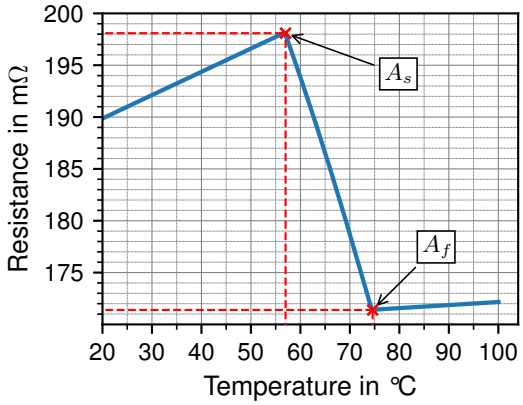

Fig. 5: Phase- and temperature-dependent resistance of the SMA wire

whereby the resistance can be interpreted as a functional indicator of the global actuator state.

The time scales of the simulated activation range from sub-hertz to low hertz, corresponding to the heating and cooling processes typical for shape memory wires. Against this background, the selected sensor technology is suitable for consistently recording both the mechanical deflection and the electrical signal over time. The simulation is not intended to predict the actual system behaviour exactly, but rather to estimate relevant measuring ranges, sampling rates and signal magnitudes for the designed test setup.

At the same time, it must be taken into account that the measured electrical resistance represents an effective average value over the length of the wire and cannot resolve local temperature or conversion states. This limitation is acceptable for the pursued goal of a conceptual, sensorless measurement approach, since the resistance is used as a calibrated state variable to describe the global activation and conversion state.

Conclusion and further work

The simulations carried out show that the temperature-induced phase transition of a shape memory wire integrated into a structure leads to reproducible mechanical actuation and that the activation and transition state is also reflected in the electrical resistance. The numerical results confirm that the selected sensor technology and the designed measurement setup are suitable for reliably recording the relevant mechanical and electrical variables in the dynamic range expected in the experiment.

The next step is to implement and validate the proposed measurement setup experimentally. In particular, the relationship between electrical resistance, temperature and mechanical deflection will be calibrated experimentally, and the influence of temperature gradients and hysteresis effects will be investigated.

References

[1] S. Langbein and A. Czechowicz, *Formgedächtnistechnik: Entwickeln, Testen und Anwenden*. Wiesbaden: Springer Fachmedien, (2021)

[2] M. N. Islam, M. B. Gonzalez, S. Tabassum, and K. M. M. Billah, "3d printed shape memory alloy wire embedded actuator," in *2024 IEEE 17th Dallas Circuits and Systems Conference (DCAS)*, ISSN: 2766-5186, (2024), pp. 1–5; doi: 10.1109/DCAS61159.2024.10539916

[3] G. Stano, S. M. A. I. Ovy, J. R. Edwards, M. Cianchetti, G. Percoco, and Y. Tadesse, "One-shot additive manufacturing of robotic finger with embedded sensing and actuation," *The International Journal of Advanced Manufacturing Technology*, vol. 124, no. 1, pp. 467–485, (2023); doi: 10.1007/s00170-022-10556-x

[4] Metastat Insight and Technologies Pvt. Ltd. "Shape memory alloy market size & share report by 2031," Metastat Insight, Accessed: Feb. 21, 2025. [Online]. Available: https : / / metastatinsight.com

[5] M. Hübler, *Methodik zur Auslegung und Herstellung von aktiven SMA-FKV-Hybridverbunden*. Technische Universität Kaiserslautern, (2016)

[6] A. Hein, *Auslegung und Entwurf adaptiver Strukturen und Systeme mit Formgedächtnislegierungen*. Stuttgart : Institut für Konstruktionstechnik und Technisches Design, (2021)

[7] T. M. Wendt, A. Dierle, T. Seifert, and A. Schnebel, "C4.2 - novel characterisation and modeling of the thermal behavior of multi-wire SMA actuators for robot grippers," *Lectures*, pp. 153–154, (2025); doi: 10.5162/SMSI2025/C4.2

[8] A. Dierle, T. M. Wendt, and T. Seifert, "Integration of shape memory alloy wires into additive fabricated structures for robotic grippers," in *Proceedings of the XI ECCOMAS Thematic Conference on Smart Structures and Materials (SMART 2025)*, in press, (2025)

[9] DYNALLOY Inc. "Technical characteristics of FLEXINOL® actuator wires," DYNALLOY Inc. Accessed: Dec. 15, 2025. [Online]. Available: https://dynalloy.com/wp-content/uploads/2025/03/TCF1140.pdf

[10] "Nitinol linear actuator (2 way) shape memory alloy wire," Nexmetal Corporation, Accessed: Dec. 23, 2025. [Online]. Available: https : / / nexmetal.com/products/nitinol-linear-actuator

[11] S. Sławski, M. Kciuk, and W. Klein, "Change in electrical resistance of SMA (NiTi) wires during cyclic stretching," *Sensors (Basel, Switzerland)*, vol. 22, no. 9, p. 3584, (2022); doi: 10.3390/s22093584

[12] D. Scholtes, S. Seelecke, and P. Motzki, "Electro-thermo-mechanical characterization of shape memory alloy wires for actuator and sensor applications—part 1: The effects of training," *Engineering Reports*, vol. 6, no. 10, e12867, (2024); doi: 10.1002/eng2.12867

[13] "3D goes HD - ECCO 75 Series high resolution laser sensors," SmartRay, Accessed: Sep. 1, 2025. [Online]. Available: https://www.smartray.com/de/3d-sensoren/ecco-75-100/

[14] H. Song, E. Kubica, and R. Gorbet, "Resistance modelling of shape memory alloy wires," *e-Journal of Nondestructive Testing*, vol. 17, no. 2, (2012)

[15] "COMSOL 6.3 - shape memory alloy," Accessed: Mar. 25, 2026. [Online]. Available: https://doc.comsol.com/6.3/doc/com.comsol.help.sme/sme_ug_theory.06.041.html#3685019